3-D Magneto-Mechanical Finite Element Analysis of Galfenol-Based Energy Harvester Using an Equivalent Stress Model

U. Ahmed [1], U. Aydin [2], L. Daniel [3,4], and P. Rasilo [1]

[1]Unit of Electrical Engineering, Tampere University, FI-33720 Tampere, Finland
[2]ABB Oy, Marine and Ports, FI-00980 Helsinki, Finland
[3]Laboratoire de Génie Electrique et Electronique de Paris, CNRS, CentraleSupélec,
Université Paris-Saclay, 91192 Gif-sur-Yvette, France
[4]Laboratoire de Génie Electrique et Electronique de Paris, CNRS, Sorbonne Université, 75252 Paris, France

This article presents the implementation of an equivalent stress model to analyze a Galfenol-based magneto-mechanical energy harvesting concept device. The equivalent stress approach can transform any arbitrary stress tensor into a uniaxial stress acting along the direction of the magnetic flux density. Unlike multiaxial magneto-mechanical phenomenological models, it offers simple implementation to predict the permeability change by interpolation from uniaxial measurements. For the first time, the proposed model is implemented in a 3-D finite element solver using COMSOL Multiphysics software to analyze an energy harvesting setup, where the effect of mechanical preload and magnetic bias on the output power can be studied. The model is tested under different compressive loading cases ranging 20–80 MPa, and the simulated results are compared with the measurement results for validation. The results show that the approach can successfully be used as a tool to analyze the behavior of the harvester device and to determine the optimal design parameters.

Index Terms—Constitutive laws, energy harvesting, magnetoelasticity, magnetostriction, strain, stress.

I. INTRODUCTION

ANALYSIS and design of magnetostrictive energy harvesters have been widely studied in the past decade. The energy harvesters allow conversion of mechanical vibration energy into electrical energy originating from ambient vibrational sources such as buildings, bridges, rail tracks, or moving parts of machines. Such harvesters can be employed at remote locations to power up wireless sensor nodes or small-scale electronic devices [1]. After the discovery of giant magnetostrictive materials (Galfenol, Terfenol-D, Metglas, and so on), the research on magnetostrictive energy harvesting has predominantly increased and various prototype devices have been introduced as proofs of concept [2], [3].

The amount of harvested power is influenced by the operating conditions (mechanical preload and magnetic bias) and design characteristics (amplitude and frequency of vibration, device geometry, magnetic closure circuit, and so on). Modeling tools are required to analyze and design such devices and determine the influence of design parameters on device performance. In addition, due to 3-D multiaxial nature of magnetic field and mechanical stress, the analysis of such devices becomes quite complex [4].

Various researches have been done to model the magneto-mechanical effects of the magnetostrictive harvesters using phenomenological models [2], [3], [5]. Such models are based on deriving a more or less empirical analytical expression for the constitutive equations defining the magneto-elastic behavior of the material. Finding a practical analytical expression which sufficiently replicates the magneto-elastic behavior is difficult. Indeed, fully coupled nonlinear models are promising but complicated to implement. In addition, the analytical expression might need to be changed when the state variables change.

This article proposes to use an equivalent stress model presented in [6] for 3-D magnetodynamic analysis of a magneto-mechanical energy harvester concept device. The equivalent stress model is tested for the first time in an energy harvesting application. It offers a simple and straightforward approach that only requires measurements from the uniaxial stress-dependent magnetization curves (B–H curves). The model is implemented in COMSOL Multiphysics software for 3-D finite element (FE) simulations. This article also discusses and compares the results against the thermodynamic modeling approach developed and tested in [7]. The idea is to test how these models can be utilized for the analysis of the energy harvesting device. The simulated results from both models are compared with measurement results for validation.

II. EXPERIMENTAL METHODS

In order to validate the modeling approach and to analyze the energy harvesting device, an experimental setup is developed and tested as discussed in [8]. The experimental setup is divided into two parts. The stress-dependent magnetization curves are obtained to characterize the active material (Galfenol) in the first part, whereas the second part is developed for testing the actual energy harvester setup.
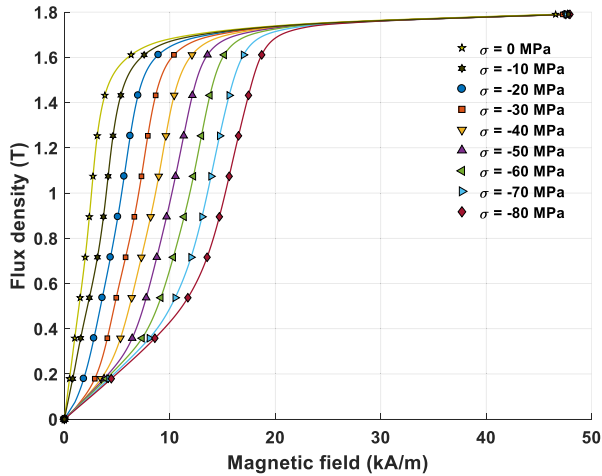
Fig. 1. Measured $B–H$ curves produced from material characterization at different mechanical preload (σ) values.

Fig. 2. Relative permeability versus magnetic flux density at different mechanical preload (σ) values.

The measurement principles are summarized in this section, while a detailed description of both setups can be found in [7].

A. Material Characterization

The characterization of Galfenol is performed first to obtain the magnetization curves ($B–H$ curves) under various static preload (σ) values. A cylindrical Galfenol rod of 60 mm in length and 12 mm in diameter is utilized as the active material for the harvester. In order to obtain the stress-dependent $B–H$ curves, the Galfenol rod is first magnetized with the help of two U-shaped cores and two coils supplied by 200 mHz AC voltage. The rod is then subjected to various static uniaxial compressive preloads σ ranging 0–80 MPa with a step of 5 MPa. The magnetic field strength H is measured using a Hall probe placed at the middle part of the sample and the magnetic flux density B is obtained by integrating the voltage induced in the pickup coil wound around the sample. Since only anhysteretic material models are considered, single-valued magnetization properties are extracted by averaging the ascending and descending branches of the measured hysteresis loops in the H direction. The characterization produces a set of magnetization curves $B(H)$ as a function of the static uniaxial stress σ presented in Fig. 1, from which we can interpolate the permeability as $\mu(B, \sigma)$, as shown in Fig. 2.

B. Energy Harvester Setup

The schematic of the prototype energy harvester setup is presented in Fig. 3(a). In this setup, the Galfenol rod is magnetized with the help of cylindrical NdFeB permanent magnets (PMs) and four L-shaped cores, as shown in Fig. 3(b). The magnets have physical dimensions of 12 mm in diameter and 6 mm in thickness with a remanence flux density of $B_r = 1.1$ T and a coercivity of $H_c = 995$ kA/m and produce a magnetic bias into the sample. The Galfenol rod is machined to reduce the diameter of the sample to 6 mm from the middle for the length of 48 mm as seen from Fig. 3(a). A pickup coil
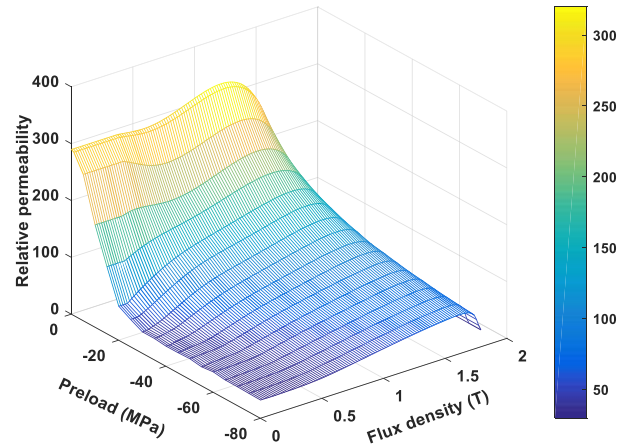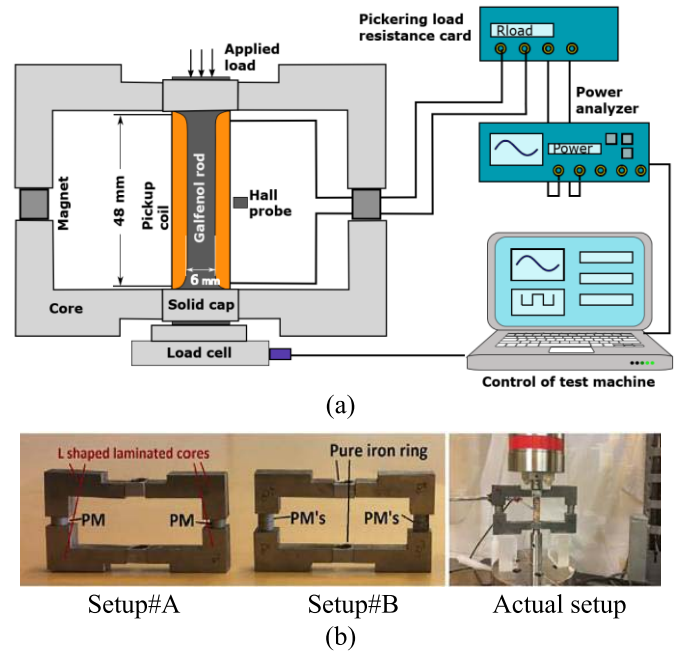

Fig. 3. Schematic of the (a) energy harvester setup and the (b) actual setup with both configurations Setup#A (two magnets) and Setup#B (four magnets).

consisting of 2000 turns of 0.2 mm wire is wound around the machined sample. Since the test machine could exert a maximum sinusoidal force of 7 kN rms (10 kN peak), machining the sample allowed us to operate at large range of stress values. A programmable precision load resistance card PXI 40-297-002 is connected to the pickup coil as variable load resistance to measure the output power.

To analyze the effect of magnetic bias, two different magnetizing configurations were studied (Fig. 3(b)). Setup#A contains one PM at each column of the L-shaped core (two magnets in total), whereas Setup#B has two magnets (PMs) on each column (four magnets in total). For the energy harvester setup, the Galfenol rod is first subjected to a static compressive preload σ followed by sinusoidal dynamic load $\Delta\sigma$ of 8 MPa

at 100 Hz vibration frequency. The application of the dynamic load causes an induced voltage in the pickup coil due to Villari effect and Faraday's law. Finally, the output power supplied to the load resistance of 160 Ω is measured.

The experiment is repeated for various mechanical preload σ values ranging from 20 to 80 MPa keeping the dynamic load $\Delta\sigma$ and vibration frequency constant. The same experiment is repeated for both configurations Setup#A and Setup#B to determine the effect of mechanical preload and magnetic bias over the output power. The aim of this article is to test the equivalent stress model to predict the output power as a function of mechanical preload and magnetic bias and compare the results with the measurements obtained from the harvester.

III. MODELS

A. Equivalent Stress Model

The idea of equivalent stress models is to utilize the permeability data $\mu(B, \sigma)$ obtained from the uniaxial measurements to interpolate the correct permeability for a combination of an arbitrary flux-density vector $\boldsymbol{B}$ and stress tensor $\boldsymbol{\sigma}$. This is done by converting the stress tensor into an equivalent uniaxial stress σ_{eq} along the direction of the magnetic flux density in such a way that similar macroscopic magneto-elastic behavior of the material is obtained. The complete derivation of the equivalent stress/strain model is presented in [6]. The magnetic flux density vector is written as $\boldsymbol{B} = B\boldsymbol{b}$, where B is the magnitude and $\boldsymbol{b}$ the direction vector. The equivalent stress in terms of magneto-elastic energy can be written as

$$\sigma_{eq} = \frac{3}{2}\boldsymbol{b}^{\mathrm{T}}\boldsymbol{s}\boldsymbol{b}, \tag{1}$$

where $\boldsymbol{s} = \boldsymbol{\sigma} - (1/3)\mathrm{tr}(\boldsymbol{\sigma})\boldsymbol{I}$ is the deviatoric part of the stress tensor $\boldsymbol{\sigma}$ and $\boldsymbol{I}$ is the identity matrix.

B. Thermodynamic Magneto-Mechanical Model

In addition to measurements, the equivalent stress approach is compared with a COMSOL implementation of a thermodynamic modeling approach discussed in [7]. In brief, a fully 3-D directly coupled multiaxial magneto-mechanical model is obtained by analytically expressing a Helmholtz free energy as a function of the magnetic flux-density vector $\boldsymbol{B}$ and strain tensor $\boldsymbol{\varepsilon}$ as

$$\psi(\boldsymbol{B}, \boldsymbol{\varepsilon}) = \frac{1}{2}\lambda I_1^2 + \mu I_2 + \sum_{i=1}^{\eta_\alpha}\alpha_i I_4^i + \sum_{i=1}^{\eta_\beta}\beta_i I_5^i + \sum_{i=1}^{\eta_\gamma}\gamma_i I_6^i, \tag{2}$$

where $I_1 = \mathrm{tr}(\boldsymbol{\varepsilon})$, $I_2 = \mathrm{tr}(\boldsymbol{\varepsilon}^2)$, $I_4 = \boldsymbol{B} \cdot \boldsymbol{B}$, $I_5 = \boldsymbol{B} \cdot \boldsymbol{eB}$, and $I_6 = \boldsymbol{B} \cdot \boldsymbol{e}^2\boldsymbol{B}$; λ and μ are Lamé parameters obtained from Young's modulus and Poisson's ratio; and α_i, β_i, and γ_i are fitting parameters. The magnetic field strength vector $\boldsymbol{H}$ and stress tensor $\boldsymbol{\sigma}$ are obtained by partial differentiation of the free energy density as

$$\boldsymbol{H}(\boldsymbol{B}, \boldsymbol{\varepsilon}) = \left(\frac{\partial\psi}{\partial\boldsymbol{B}}\right)^{\mathrm{T}} \text{ and } \boldsymbol{\sigma}(\boldsymbol{B}, \boldsymbol{\varepsilon}) = \frac{\partial\psi}{\partial\boldsymbol{\varepsilon}}. \tag{3}$$

In order to obtain the material parameters α_i, β_i, and γ_i, the magnetization curves obtained from (3) are fitted against
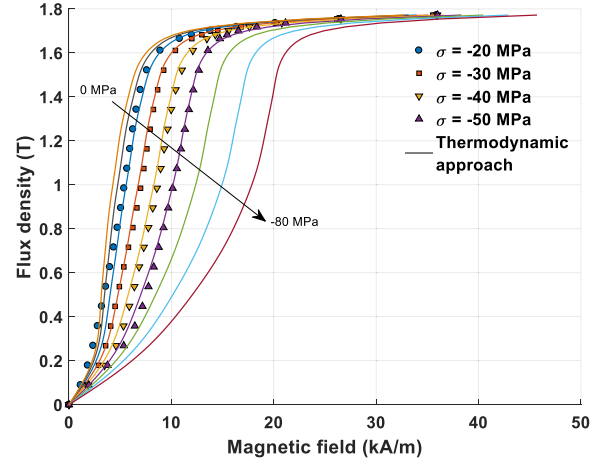

Fig. 4. Simulated magnetization curves under mechanical preload values of 0, -10, ..., -80 MPa using the thermodynamic approach. The markers denote the measurements used for fitting the model.

the uniaxial measurement $H(B, \sigma)$ for the mechanical preload range 20–50 MPa for $\eta_\alpha = 11$, $\eta_\beta = 1$, and $\eta_\gamma = 2$. The B–H curves produced by the thermodynamic model in the range of 0–80 MPa are presented in Fig. 4. A relatively good fitting can be achieved in a narrow stress range, but outside of the fitting data range (below 20 MPa and above 50 MPa), the simulated results deviate from the measurements shown in Fig. 1.

IV. FE MODEL

The analytical expression of the equivalent stress σ_{eq} is implemented in COMSOL Multiphysics software for 3-D FE simulation of the prototype device discussed in Section II-B. Due to symmetry reasons, modeling 1/8th of the geometry is sufficient. At first step, a purely mechanical simulation with linear elasticity is performed to calculate the stress distribution in the Galfenol rod by solving $\nabla \cdot \boldsymbol{\sigma} = 0$ with the applied load imposed as a Neumann boundary condition on the top of the rod. The stress tensor only includes the stress from the mechanical loading written as $\boldsymbol{\sigma} = \mathbf{C}:\boldsymbol{\varepsilon}$, where $\mathbf{C}$ is the fourth-order mechanical stiffness tensor and $\boldsymbol{\varepsilon}$ is the pure elastic strain tensor.

At second step, an electromagnetic simulation is performed which uses the equivalent stress model for the permeability as the constitutive law as $\boldsymbol{H}(\boldsymbol{B}, \boldsymbol{\sigma}) = \boldsymbol{B}/\mu(||\boldsymbol{B}||, \sigma_{eq})$, where $\boldsymbol{B} = \nabla \times \boldsymbol{A}$. The COMSOL utilizes the local permeability $\mu(||\boldsymbol{B}||, \sigma_{eq})$ interpolated from the uniaxial permeability measurements shown in Fig. 2. In the actuator material, the combination of Ampere's and Faraday's laws is solved in terms of the magnetic vector potential $\boldsymbol{A}$ as

$$\nabla \times \boldsymbol{H}(\boldsymbol{B}, \boldsymbol{\sigma}) + \kappa\frac{\partial\boldsymbol{A}}{\partial t} = 0, \tag{4}$$

where κ denotes the electrical conductivity. In the other regions, a purely electromagnetic problem is solved as

$$\nu\nabla \times \nabla \times \boldsymbol{A} + \kappa\frac{\partial\boldsymbol{A}}{\partial t} = \boldsymbol{J}_s + \nabla \times \boldsymbol{H}_c, \tag{5}$$

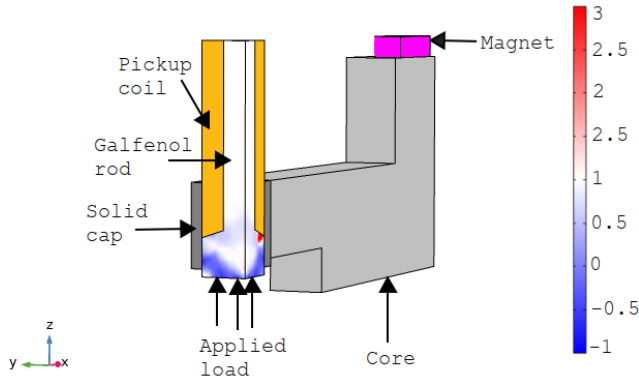where ν is the constant reluctivity. The circumferential source current density in the pickup coil of N turns is

Fig. 5.   Distribution of the stress ratio $\sigma_{\mathrm{eq}}/\sigma_{zz}$ in the Galfenol rod.

Fig. 6.   Measured and simulated output power for different mechanical preload values and the effect of preload over magnetic bias.

$J_s = (Ni_{\mathrm{coil}}/S_{\mathrm{coil}})e_\theta$, where i_{coil} and S_{coil} are the coil current and coil cross section area. The electrical conductivity κ is nonzero only in the PMs and the solid caps connecting the rod and core (Fig. 3(a)), while H_{c} is the coercive field of the magnets.

The power flow from the pickup coil to the load resistance is modeled using the electric circuit interface in COMSOL, calculating the pickup coil current from

$$\frac{N}{S_{\mathrm{coil}}} \int_{V_{\mathrm{coil}}} \frac{\partial A_\theta}{\partial t} dV + (R_{\mathrm{coil}} + R_{\mathrm{load}})i_{\mathrm{coil}} = 0, \qquad (6)$$

where $R_{\mathrm{coil}} = 32.6\ \Omega$ is the coil resistance, and the first term represents the back emf computed by averaging the time derivative of the circumferential component of the vector potential over all possible paths in the coil volume V_{coil}. The time integration is done using Backward-Euler method, and the resulting nonlinear system is solved using the Newton-Raphson iteration. The implementation of the thermodynamic model in COMSOL Multiphysics software for 3-D FE simulation is discussed in [7].

V. Results and Discussion

Due to the axial loading, the stress in the whole Galfenol rod is mainly uniaxial, so that the zz-component dominates. In the middle part of the rod, the flux density is oriented parallel to the stress. However, near the end of the rod, the flux density turns toward the core, causing the magneto-mechanical problem to become multiaxial. This is seen in Fig. 5, where the distribution of the ratio $\sigma_{\mathrm{eq}}/\sigma_{zz}$ between the equivalent stress and the zz-component of the stress tensor is visualized. Using the equivalent stress model for correctly interpolating the permeability in the regions close to the core is thus justified.

The energy-harvesting simulations are carried out using a load resistance of 160 Ω at a constant dynamic load $\Delta\sigma = 8$ MPa and mechanical vibration frequency of 100 Hz. The influence of operating conditions (mechanical preload and magnetic bias) over the output power is simulated by varying the operating conditions. The simulated results are compared with the measured ones for validation. The results are simulated for the preload range of 20–80 MPa since we are
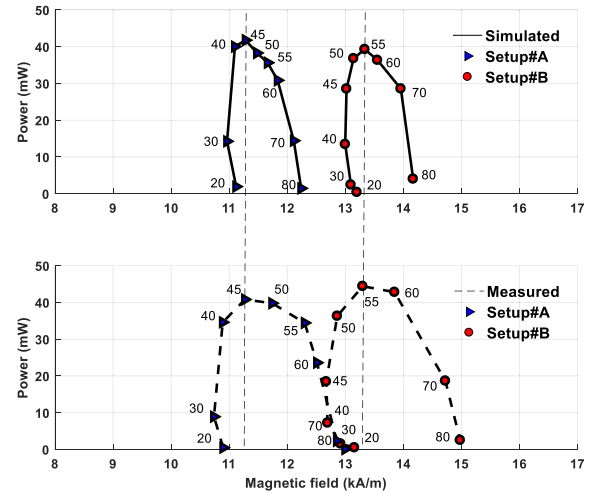
mainly interested in the range where we obtain the maximum output power.

It was observed that the output power is very sensitive to variations in the magnetic bias and changes significantly if the magnetic field bias changes slightly under a constant mechanical preload. It is difficult to predict the magnetic bias accurately with the FE model due to the existence of small clearances between the cores and the sample and the inaccuracies in modeling the magnetization properties of the core, which affect the total reluctance of the flux path. In order to allow a reasonable comparison of the output powers under different mechanical preloads, the remanence flux density of the PMs is tuned so that the magnetic field near the middle part of the sample matches the field measured with the Hall-probe under the mechanical preload value at which the maximum output power is obtained. The remanence is then kept constant when other mechanical preload values are simulated. The influence of the mechanical preload on the magnetic bias as well as the sensitivity of the output power to the magnetic bias can be seen from Fig. 6. The tuning is done for the preload value of 45 MPa for Setup#A and 55 MPa for Setup#B indicated by vertical-dashed lines. The magnetic bias changes due to the applied preload which is evident from both measured and simulated results in Fig. 6.

For both the models, the comparison among measured and simulated average output powers for both configurations of the harvester setups (Setup#A and Setup#B) is presented in Fig. 7. The results indicate that the equivalent stress model can predict the output power with reasonable accuracy. The simulated results are consistent with the measured results with peak power occurring at 45 MPa for Setup#A and 55 MPa for Setup#B.

For comparison, the results obtained from the directly coupled COMSOL Multiphysics implementation of the thermodynamic constitutive model described in [7] are presented in Fig. 7. The model predicts slightly larger values when compared with measured ones but can correctly estimate the mechanical bias at which maximum power is obtained. Moreover, the simulated results follow similar trends of the
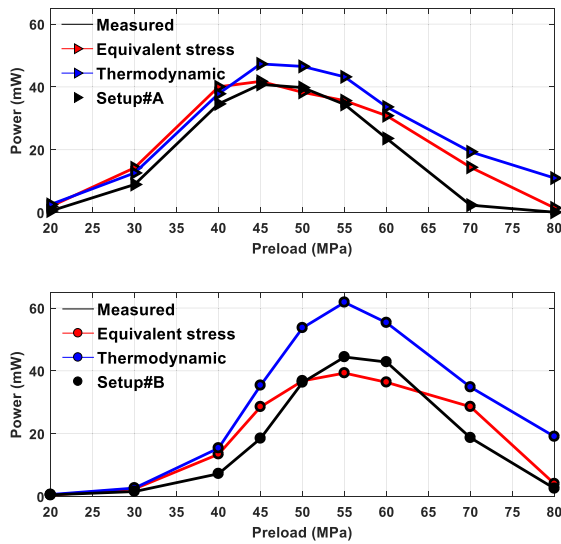
Fig. 7. Measured and simulated average output power at varying operating conditions using both equivalent stress and thermodynamic modeling approach.

measurement results where the maximum power occurs at 45 MPa for Setup#A case and 55 MPa for Setup#B.

The limitation of the thermodynamic modeling technique is that it is unable to properly fit to the measured magnetization curves for wide range of static mechanical preload cases. The discrepancies can be seen by comparing the measured and simulated B–H curves in Figs. 1 and 4, respectively. The simulated results vary by the choice of the σ values used when fitting the model, as well as the degree of polynomial coefficients for parameters α, β, and γ. The limitation of the equivalent stress model is that it does not consider the stress due to magnetostriction and thus the total simulated stress is less than the actual stress which affects the simulated magnetic field bias as seen from Fig. 6.

The difference between measured and simulated results can be explained by the limitations of the models and partly due to the uncertainty and repeatability of the measurements. The measurements were found sensitive to the warm-up time and alignment of the harvester to the vertical loading system. These parameters affect the repeatability of the measurements and must be kept constant.

VI. CONCLUSION

In this article, the equivalent stress model is successfully implemented and tested for an energy harvester setup. The 3-D FE simulations are carried out using commercially available software COMSOL Multiphysics, and the simulated results are compared with measurement results for validation. The results show that the model can successfully predict the maximum output power and mechanical preload and thus can be employed to analyze the harvester device.

The simulated results from the equivalent stress model are also compared with those from a directly coupled FE model implemented using a thermodynamic approach. The main advantage of the equivalent stress model is that, unlike in the thermodynamic approach, there are no free parameters that would require fitting against measured B–H curves and the model is quite simple to implement.

Since the energy harvesters are excited by ambient vibration sources, the excitation amplitude and frequency cannot be controlled. The equivalent stress model can provide the knowledge of the optimal operating conditions (mechanical preload and magnetic bias), which can be tuned to design the harvester geometry tailored to the specific application (powering wireless sensor node or RF tag). We are mainly interested in the preload range (45–60 MPa) where the studied material provides the maximum output power density. In this stress region, the accuracy of the equivalent stress model is sufficient.

The uncertainties related to material properties and manufacturing tolerances make it difficult to accurately predict the magnetic bias using the FE models. This is not necessarily a major problem for engineering design, thanks to the dependence of optimal mechanical preload on the magnetic bias [8]. If the magnetic bias in a manufactured energy harvester differs from the design value, the mechanical preload can be adjusted to change the operation point so that the maximum output power is obtained.

REFERENCES

[1] L. Wang and F. G. Yuan, "Vibration energy harvesting by magnetostrictive material," *Smart Mater. Struct.*, vol. 17, no. 4, Aug. 2008, Art. no. 045009.

[2] C. S. Clemente and D. Davino, "Modeling and characterization of a kinetic energy harvesting device based on galfenol," *Materials*, vol. 12, no. 19, p. 3199, Sep. 2019.

[3] C. S. Clemente, A. Mahgoub, D. Davino, and C. Visone, "Multiphysics circuit of a magnetostrictive energy harvesting device," *J. Intell. Mater. Syst. Struct.*, vol. 28, no. 17, pp. 2317–2330, Oct. 2017.

[4] C. Mudivarthi, S. Datta, J. Atulasimha, and A. B. Flatau, "A bidirectionally coupled magnetoelastic model and its validation using a galfenol unimorph sensor," *Smart Mater. Struct.*, vol. 17, no. 3, Jun. 2008, Art. no. 035005.

[5] B. Rezaeealam, "Finite element analysis of magnetostrictive vibration energy harvester," *COMPEL-Int. J. Comput. Math. Electr. Electron. Eng.*, vol. 31, no. 6, pp. 1757–1773, Nov. 2012.

[6] O. Hubert and L. Daniel, "Energetical and multiscale approaches for the definition of an equivalent stress for magneto-elastic couplings," *J. Magn. Magn. Mater.*, vol. 323, no. 13, pp. 1766–1781, Jul. 2011.

[7] U. Ahmed, U. Aydin, M. Zucca, S. Palumbo, R. Kouhia, and P. Rasilo, "Modeling a Fe-Ga energy harvester fitted with magnetic closure using 3D magneto-mechanical finite element model," *J. Magn. Magn. Mater.*, vol. 500, Apr. 2020, Art. no. 166390.

[8] S. Palumbo, P. Rasilo, and M. Zucca, "Experimental investigation on a Fe-Ga close yoke vibrational harvester by matching magnetic and mechanical biases," *J. Magn. Magn. Mater.*, vol. 469, pp. 354–363, Jan. 2019.